A NOVEL CLOSED FORM SOLUTION FOR ULTRASOUND CALIBRATION

Emad Boctor, Anand Viswanathan, Michael Choti,
Russell H. Taylor, Gabor Fichtinger, and Gregory Hager

Engineering Research Center for Computer Integrated Surgical Systems and Technology
Johns Hopkins University, http://cisstweb.cs.jhu.edu
eboctor@ieee.org, {anand, rht, Gabor, and Hager}@cs.jhu.edu

ABSTRACT

This paper describes a new robust method for calibration of ultrasound probe (2D/3D). Prior to calibration, a position sensor is attached to the probe for tagging each image/volume with its position and orientation in space. The localization process of the acquired image/volume in 3D space critically requires a calibration procedure that determines its accuracy. The calibration procedure is performed to determine the transformation (translations, rotations, scaling) of the scan plan with respect to the position sensor. In the literature, there are many solutions to the US calibration, but no approach has been published so far that brings a closed form solution for this problem. The proposed methodology will provide a closed form solution from two motions of the US probe. Also, we are presenting the calibration setup along with the experiments that have been conducted with synthetic and real sequences. This calibration method is shown to be easy and fast to perform.

1. INTRODUCTION

During the past two decades surgical procedures have witnessed a revolutionary change, nowadays referred to as Computer Integrated Surgery. Especially with the introduction of various imaging modalities, like Magnetic Resonance Imaging (MRI), Computer Tomography (CT), and Ultrasound (US), surgical procedures have seen advancement in all stages, pre-, post-, and –intra-operative alike. True 3D imaging modalities, like MRI and CT, are extremely potent in terms of their rendering capabilities, but are cumbersome to use for intra-operative procedures, mainly due to obstructive hardware and imaging latency. US, however, has been emerging as a widely popular image guidance modality, since it is real-time, convenient to use in the operating room, and readily inexpensive compared to CT and MRI. Significant amount of research has been conducted to convert US technology to provide the physicians with a 3D real-time visualization of the internal anatomy [1]. Currently, there are three strategies to acquire 3DUS dataset: freehand, mechanical sweeping of 2D probe, and electronical sweeping (3D probe.) Using US as a guidance modality for surgical procedures would require tracking the imaging probe with a magnetic or optical tracking device. In this case, a fixed transformation between the US beam and the tracking device needs to be determined, so that arbitrary image pixels can be referenced in a global frame. Obtaining this fixed transformation is referred to as "ultrasound calibration". After calibration, a 3D volume is reconstructed by some surface- or voxel-based method, and then the data is visualized with some appropriate combination of surface extraction, volume rendering, re-slicing, panoramic viewing, or multi-planar techniques. Apparently, the accuracy of calibration greatly influences the quality of the reconstructed volume and visualization, through these the accuracy and realty of surgical planning and monitoring.

The calibration procedures are mainly search algorithms for the unknown transformation parameters to maximize the similarity between the acquired US images in phantom space and the phantom model (image or geometrical model). There is error associated with each stage of the process (phantom fabrication, image acquisition, spatial co-registration, image processing, formulation, and numerical optimization solution), the combined total error of which may easily amount to a large degree.

Geometrical model based phantoms like points [2, 3, 4, 5, 6], plane [7, 4, 6] exist and some studies have compared their accuracy and performance [4, 6]. The cross-wire and three-wire phantoms require long time of acquisition and are hard to automate, while the single-wall phantom as in Cambridge phantom [4] is automatic repeatable method. Figure 1 shows a typical formulation for the coordinate systems required for mentioned phantoms.

0-7803-8388-5/04/$20.00

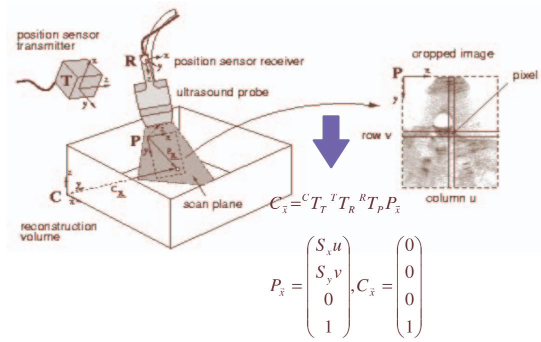

Figure 1: The chain of transformations is from pixel frame P, to the receiver frame R, to transmitter frame T, and finally to construction frame C. The (u,v) pixel coordinates are multiplied by (S_x,S_y) scale factors. The resulting transformed point C_x has the (0,0,0) coordinate values [Cross-wire Phantom]. (Upper figure Courtesy of R. Prager)

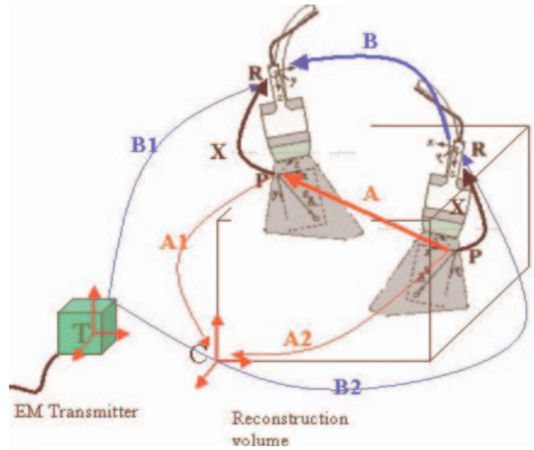

Figure 2: The coordinate systems formulation for the proposed AX =XB method.

Other groups such as Vanderbilt University [8] use pointer-based methods, which simplify the nonlinear optimization problem. However, the method requires pointer calibration and careful data collection. One variation of the point-based method was introduced by Pagoulatos [5], where the phantom is a collection of N-shaped fiducials that are defined in the tracker frame.

Blackall et al. [9] presented a voxel based registration method for US calibration. Registration is achieved by the maximization of normalized mutual information. This happened when accurate calibration parameters give optimal similarity between the US images of the phantom and the 3D voxel based model.

In this paper (section 2), the US calibration framework in figure 1 is integrated into the AX = XB framework as in figure 2, using a recent closed form solution [10] for the "AX = XB" problem. In section 3, there is a description of the details of the calibration setup, which is composed of the US machine, the optical tracking device and the phantom used to recover the "A". In addition, the results from synthetic experiments and real US sequences will be discussed in section 4.

2. CLOSED FORM FORMULATION

Figure 2 presents the coordinate systems of the new formulation. A_1, A_2 are the transformations of US image coordinate system (*P*) with respect to the reconstruction coordinate system (*C*) at poses 1 and 2 respectively. From A_1, A_2, we have the transformation between US image coordinate system at pose 1 and 2, $A = A_2A_1^{-1}$. This transformation frame A, could be recovered using a calibration phantom to determine both A1, A2, or recovered directly from registering the US image 2D to a prior 3D model for the object being scanned. A version of the N-shaped phantom was used to identify "A". B_1, B_2 are the tracking device readings for the sensor frame (*R*) with respect to tracker reference frame (*T*) at poses 1 and 2 respectively. Again the relative pose between sensor frame (*R*) at pose 1 and 2 is given by $B = B_2^{-1}B_1$. This yields the following homogeneous matrix equation:

$$AX = XB \qquad (1)$$

Where A is estimated, B is assumed to be known and X is the unknown transformation between the US image coordinate system and the sensor frame (*R*). The estimated US image frame motion in general is given by:

$$A(\lambda) = \begin{pmatrix} & & & \lambda_x u_{ax} \\ & R_a & & \lambda_y u_{ay} \\ & & & \lambda_z u_{az} \\ 0 & 0 & 0 & 1 \end{pmatrix} \qquad (2)$$

Where R_a is the rotation of the US image frame between pose 1 and 2, λ is the unknown scale factor vector that relates the translation u_a in voxel space (3DUS, CT, or MRI) to the US image frame translation t_a (in mm) such that

$$t_a = \begin{pmatrix} \lambda_x u_{ax} \\ \lambda_y u_{ay} \\ \lambda_z u_{az} \end{pmatrix} = \begin{pmatrix} u_{ax} & 0 & 0 \\ 0 & u_{ay} & 0 \\ 0 & 0 & u_{az} \end{pmatrix} \cdot \begin{pmatrix} \lambda_x \\ \lambda_y \\ \lambda_z \end{pmatrix} = D_{ua}\lambda. \qquad (3)$$

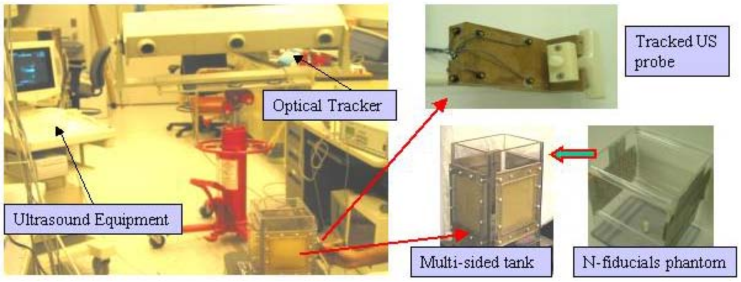

Figure 3: Calibration setup shows the multi-sided tank with the N-fiducials

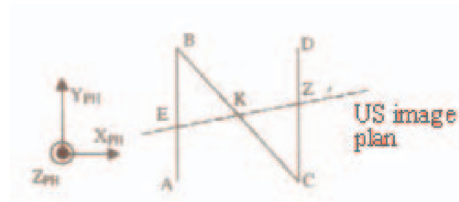

Figure 4: The N based phantom helps in extracting the pose between the US image plan and the phantom space, "A1 transformation"

It is important to account for the most general case where the scale factor λ that converts from voxel space to mm space is not known. Such scenario could happen if "*A*" is recovered by registering the US image to a prior acquired model in voxel space. From the homogeneous equation (1) and using (2), one obtains:

$$R_a R_x = R_x R_b \tag{4}$$

$$R_a t_x + D_{ua}\lambda = R_x t_b + t_x \tag{5}$$

In the linear formulation of the problem we will use the linear operator *vec* and the Kronecker product (⊗)[11]. Using the following fundamental property of the Kronecker product:

$$vec(CDE) = \left(C \otimes E^T\right) vec(D) \tag{6}$$

One can rewrite (4) and (5) into:

$$\left(R_a \otimes R_b\right) vec\left(R_x\right) = vec\left(R_x\right) \tag{7}$$

$$\left(I_3 \otimes t_b^t\right) vec\left(R_x\right) + \left(I_3 - R_a\right) t_x - D_u \lambda = 0 \tag{8}$$

From (7) and (8), we can transform the whole problem (AX=XB) into a single homogeneous linear system:

$$\begin{bmatrix} I_9 - R_a \otimes R_b & 0_{9*3} & 0_{9*3} \\ I_3 \otimes t_b^t & I_3 - R_a & -D_u \end{bmatrix} \begin{pmatrix} vec\left(R_x\right) \\ t_x \\ \lambda_{3*1} \end{pmatrix} = \begin{pmatrix} 0_{9*1} \\ 0_{3*1} \end{pmatrix} \tag{9}$$

The solution for this homogeneous linear system could be given by finding the null space, which is a subspace in R^{15}. Then the unique solution could be extracted from the null space using the unity constraint to the first 9 coefficients representing the R_x. Another way is to solve this system into two steps, first extract the rotation and then solve for the translation and scale. The complete algebraic analysis for this problem (where the scale facto is assumed to be constant in three direction) is given in [10], where it is proved that two independent motions with non-parallel axes is sufficient to recover a unique solution for AX=XB.

3. CALIBRATION SETUP

The Calibration setup as shown in figure 3, consists of a transparent plastic water tank, in which we can scan the submerged phantom (Cross-wire, Hopkins-phantom, N-based phantom) not just from the top, but also from all four sides of the tank through rubber windows [6]. We use a linear array (7.5 MHz) US probe with a rigid attachment containing optical markers tracked by an Optotrak. The actual phantom consists of a matrix of N shaped wires stretching across two parallel plates. The phantom is oriented in the multi-window tank in an oblique position so that the structure can be scanned through two opposite windows and the top, with a plurality of wires visible from each image. Similar to the work of Pagoulatos [5], an additional group of vertical N-shaped fiducials has been added to his original design and utilizes an algorithm to select the image points and relate them to points on the physical phantom space.

In relating the phantom space coordinate system to the ultrasound image space, the N shape wires provide 3 points (ellipses) for each N shape fiducial. In figure 4, E, K and Z are the 3 points that would be seen in the ultrasound image while points A,C and B,D represent points where the wire intersects the parallel plates.

Using triangle similarity and a-priori knowledge of the vertices in phantom space, the x and y coordinates of the center image point of the N shape fiducial can be computed. The location of this point K in phantom space is extracted as follows:

$$x_k = x_b + \left(\frac{KE}{EZ}\right) * \left(x_c - x_b\right)$$

$$y_k = y_b + \left(\frac{KE}{EZ}\right) * \left(y_c - y_b\right)$$

The transformation between the ultrasound image space and phantom space is then determined by using Horn's quaternion rigid registration method.

4. EXPERIMENTS AND RESULTS

Two different sets of experiments have been designed to test the calibration technique. The first set of experiments use synthetic data where optimal parameters are exactly known. The second set of experiments use real ultrasound sequences as described in section 3.

Simulation trials provides insight to the numerical behavior of the linear formulation of AX = XB, as well as a means of testing the validity of the algorithm in a controlled environment. Ultrasound noise and beam width problem would affect the accuracy of the estimated A matrix. Accordingly, the following protocol aims to simulate these disturbances. First, the missing transformation X is picked by a random choice. Second, a sequence of probe motions (sensor) is chosen. From the unknown transformation X, the ultrasound image motion can be deduced. Third, Noise is added to the ultrasound image motion frame to simulate real environment. Then running the algorithm to recalculate the X under different noise conditions as shown in table 1.

In the second set, after gathering 7 poses, the algorithm utilizes a combination of 3 of these poses. Table 2 reports the average recovered pose values as well as the standard deviation. Much of the 1.54 mm position error is attributed to the crudely prototyped of US probe attachment producing mechanical sag and limiting the angular range of tracking. Work is also underway to compare our method to crosswire technique. However, we have proved that the novel closed form formulation recovered both translation and rotation with repeatability in the order of 1.5 mm and 1.63 degrees with 3 poses only. The estimated time from capturing these 3 poses, running the semi-automated extraction method and reporting the solution is less than 1 min.

Acknowledgements: The authors acknowledge the support of the NSF grant #EEC-9731478, Aloka Corporation and Greg Fisher.

	Average Error (mm)			Standard Dev.(mm)		
Sequence I	0.0013	-0.00113	-0.0668	0.468	0.125	0.298
Sequence II	-0.002	0.00652	0.0356	0.382	0.195	-0.109
Sequence III	0.0657	-0.0357	-0.888	8.726	2.132	4.512
Sequence IV	0.0461	-0.0160	-0.895	13.89	3.459	6.058

Table 1: The above table lists average error and standard deviation in mm the recovered translation vector for different calibration sequences. The sequences were generated using synthetic data with added noise of .5%, 1%, 5%, 10% respectively.

	Average			Standard Dev.		
Position (mm)	82.566	-87.89	35.929	0.76	1.15	1.54
Angles (deg)	5.139	1.727	-2.866	1.63	0.11	0.83

Table 2: The above table lists average pose values and average deviation in mm and degrees of recovered transformation matrix using actual ultrasound and optical tracking device data.

5. REFERENCES

[1] A. Fenster, D. B. Downey, and N. H. Cardinal, "Three Dimensional Ultrasound Imaging," *Physics in medicine and biology*, vol 46, pp. 67-99, 2001.

[2] P. R. Detmer, G. Bashein, T. Hodges, K. W. Beach, E.P. Filer, D. H. Burns, and D. E. Strandness Jr., "3D Ultrasonic Image Feature Localization based on Magnetic Scanhead Tracking: In Vitro Calibration and Validation." *Ultrasound in Med. Biol.*, 23(4):597-609, 1996.

[3] J. Carr, Surface Reconstruction in 3D Medical Imaging, Ph.D. thesis, University of Canterbury, Christchurch, New Zealand, 1996.

[4] R. W. Prager, Rohling R. N., Gee A. H., and Berman L., "Rapid Calibration for 3-D Freehand Ultrasound," *Ultrasound in Med. Biol.*, 24(6):855-869, 1998.

[5] N. Pagoulatos, D. R. Haynor, and Y. Kim, "A Fast Calibration Method for 3-D Tracking of Ultrasound Images Using a Spatial Localizer," *Ultrasound in Med. Biol.*, 27(9):1219-1229, 2001.

[6] Emad M. Boctor, A. Jain, M. Choti, Russell H.Taylor, Gabor Fichtinger, "Rapid calibration method for registration and 3D tracking of ultrasound images using spatial localizer," *Proc. SPIE Vol. 5035,p. 521-532, Medical Imaging 2003.*

[7] F. Rousseau, P. Hellier, C. Barillot, "A fully automatic calibration procedure for freehand 3D ultrasound," *In IEEE Int. Symp. on Biomedical Imaging, Washington D.C, Juillet 2002.*

[8] Diane M. Muratore, Robert L. Galloway, Jr., "Beam Calibration without a Phantom for Creating a 3D Free-hand Ultrasound System" *Ultrasound in Med. & Biol., Volume 27(11), pp1557-1566, 2001*

[9] J. M. Blackall, D. Rueckert, C. R. Maurer Jr, G. P. Penney, D. L. G. Hill, and D. J. Hawkes, "An image registration approach to automated calibration for freehand 3d ultrasound," *in Proc. of Medical Image Computing and Computer-Assisted Intervention, 2000.*

[10] Nicolas Andreff and Radu Horaud and Bernard Espiau, "Robot Hand-Eye Calibration Using Structure from Motion," *International J. of Robotics Research, 20(3), pp 228-248, 2001.*

[11] John W. Brewer, "Kronecker Products and Matrix Calculus in System Theory", IEEE Trans. Circuits and systems, 25(9) Sep.1978.